

Structure of monolayer dye films studied by Brewster angle cavity ringdown spectroscopy

Rachel N. Muir and Andrew J. Alexander*

Department of Chemistry, University of Edinburgh, West Mains Road, Edinburgh, UK EH9 3JJ. E-mail: andy.alexander@ed.ac.uk

Received 2nd January 2003, Accepted 3rd February 2003

First published as an Advance Article on the web 12th February 2003

Cavity ringdown spectroscopy of films of oxazine and malachite green dyes coated on thin borosilicate substrates is described. The method involves insertion of the substrate into the cavity at Brewster's angle to reduce reflection losses. Measured absorption features of the adsorbed dyes in the visible region 580 to 700 nm show the presence of dye aggregates. The measurement of sub-monolayers of oxazine 1 as low as 0.032 monolayers with an absorption loss per pass of 5.79×10^{-5} is demonstrated.

I. Introduction

Cavity ringdown spectroscopy (CRDS) has proven enormously successful for highly sensitive absorption measurements of gas-phase species.^{1–3} The basic principle of this method is the injection of light into a high-Q cavity, where it is trapped by highly reflecting mirrors. The rate of decay of the light intensity results from intrinsic losses of the cavity, *e.g.*, losses from the mirrors, and by absorption of gaseous species in the cavity. By measuring the decay rate of the cavity containing a gaseous absorber the absorption coefficient of the species of interest can be calculated. The method is insensitive to intensity fluctuations in the light source that are largely responsible for the limitations of conventional absorption measurements.

A few studies have demonstrated the extension of CRDS to the liquid and solid phases, by employing ingenious methods to avoid the problems of extra cavity losses due to scattering by the bulk medium. Pipino and co-workers introduced an approach that uses absorption of an evanescent wave at a point of total internal reflection (TIR).⁴ The evanescent CRDS method has been demonstrated by aligning a Pellin-Broca prism in a 2 mirror cavity,⁵ or by creating monolithic cavities that employ TIR at one or all faces of a prism.⁶ Methods that involve directly placing non-gaseous materials into a 2 mirror cavity have also been demonstrated. Meijer and co-workers studied infra-red absorption of 10–30 nm thick films of solid C₆₀ deposited onto a 3 mm thick ZnSe window that was inserted into a 2 mirror cavity.⁷ The window was aligned in a planar configuration so that reflections from the 2 surfaces of the window are returned to the cavity. Similarly, Logunov studied absorption by thin films of poly(methyl methacrylate) at around 1.3 to 1.5 μm wavelengths.⁸ Scattering losses and attenuation due to the substrate are reduced for infra-red radiation compared to shorter wavelength visible light. Kleine *et al.* studied the visible absorption of thin layers of iodine, by coating solutions of iodine in acetone onto the cavity mirrors: apparently without causing irreversible damage to the mirrors.⁹

The study of liquids using CRDS has been approached following the same methods as above. Xu *et al.* measured C–H stretching overtones of benzene using one and two quartz cuvettes oriented at Brewster's angle in a 2 mirror cavity.¹⁰ Using this method, they were able to demonstrate measurements of absorption coefficients as small as $2 \times 10^{-7} \text{ cm}^{-1}$. Zare and

co-workers built a cavity flow-cell that fills the entire optical cavity with the liquid medium of interest.¹¹ Their experiments showed that the high-reflectivity mirrors are not significantly affected by contact with a number of solvents, and they reported a minimum detectable absorption coefficient of 10^{-6} cm^{-1} .

In the present work we have extended the CRDS technique to measurements of thin-film samples into the visible region using a 2 mirror cavity to study absorption spectroscopy of various dyes adsorbed onto individual borosilicate plates aligned at Brewster's angle in the cavity. This method of Brewster angle cavity ringdown spectroscopy (BACRDS) is shown to be sensitive to the surface structure of the dye films, revealing details of absorption features that would be difficult to obtain by conventional absorption measurements.

II. Experimental

A schematic of the experimental setup is shown in Fig. 1. Pulsed radiation was produced by a dye laser (Continuum ND6000) pumped by a Nd:YAG laser (Continuum Surelite II-10). In order to obtain broad tunability over the wavelength range 580–700 nm a cocktail of Rhodamine 590, 610, DCM and LDS 698 dyes in methanol was optimized in the oscillator of the dye laser, and a diluted portion of this optimized

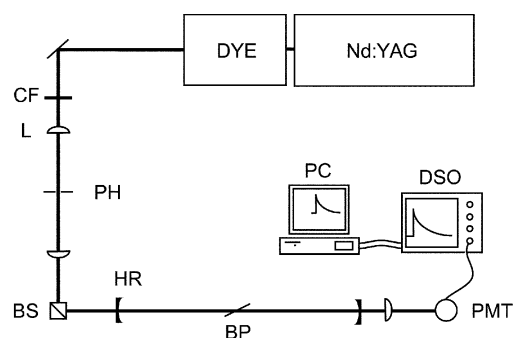


Fig. 1 Schematic diagram illustrating the experimental setup. Key: (CF) Circular neutral density filter, (L) lens, (PH) pinhole, (BS) polarizing beamsplitter cube, (HR) high reflectivity cavity mirror, (BP) brewster plate, (PMT) photomultiplier tube, (DSO) digital storage oscilloscope, (PC) personal computer.

mixture was added to the amplifier. The laser pulse duration was *ca.* 10 ns, and the output energy was *ca.* 1 mJ pulse⁻¹. The light intensity was reduced by passing through a circular variable neutral density filter and the mode was improved by spatial filtering using two matched 25 cm focal length plano-convex lenses and a 63 μm pinhole. The light was linearly polarized with a broadband polarizing beamsplitter cube, before passing into the cavity. The cavity consisted of 2 concave supermirrors (Newport 10CV00SR.30F, radius +1 m) which were mounted in precision gimbal mounts (Newport Ultima) 0.75 m apart. The measured average reflectivities of the mirrors were 99.92% per mirror at 620 nm and 99.95% per mirror at 670 nm. At the output end of the cavity, the light was captured through a 50 cm focal length lens and directed onto a photomultiplier tube (Hamamatsu PMT R928). The signal from the PMT was passed through a home-built fast preamplifier, to an 8-bit digital storage oscilloscope (Lecroy Waverunner LT342), and the trace was downloaded to a PC *via* ethernet using Labview (National Instruments). Scans over the wavelength region 580 to 700 nm were made by acquiring data every 0.3 nm, and typically averaging 10 shots per point. Ringdown traces were fitted with a single exponential decay $I = I_0 \exp(-t/\tau)$ using a nonlinear Levenberg–Marquardt method.

Malachite green, oxazine 1 and oxazine 170 laser grade dyes (Aldrich) were dissolved in analytical grade solvent, typically 12 mg in 100 mL (*ca.* 10⁻³ M). A series of solutions in the range 10⁻⁴ to 10⁻⁷ M were made from the stock solution by serial dilution, and visible spectra were recorded with a visible spectrometer (Perkin Elmer Lambda 900). Substrates used in the BACRDS experiments were 18 × 18 mm borosilicate microscope coverslip plates (Menzel Glasser MNJ-350-010K), with nominal thickness ~150 μm. These were glued with epoxy resin to a M6 screw stem, which could be mounted onto a rotary mount. Two micrometer rotary mounts were used to control the polar and azimuthal positions of the plate in the cavity. The plate was cleaned first with water and detergent, and rinsed thoroughly with de-ionized water before placing into the cavity. Once the plate was in place, the surfaces were drop-and-drag wiped with lens tissue and acetone, and the cleanliness of the plate was maximized *in-situ* by monitoring the ringdown time. The Brewster angle Θ_B for an air to glass transition is defined as:

$$\Theta_B = \tan^{-1} \left(\frac{n_{\text{glass}}}{n_{\text{air}}} \right), \quad (1)$$

where n_{air} and n_{glass} are the refractive indices of air (≈ 1) and glass (≈ 1.5) respectively, giving $\Theta_B = 56.3^\circ$. Strictly, the Brewster angle is a function of wavelength, since the refractive index n_{glass} depends on wavelength (*i.e.*, dispersion); however this changes by less than 0.2% over the wavelength range 600–700 nm. We found that alignment at Brewster angle was very easy to achieve, due to the insensitivity of the reflectivity as a function of angle.¹² By comparison, alignment of the substrate perpendicular to the light propagation direction in the cavity, as used by Engeln *et al.*⁷ and Logunov,⁸ was very difficult.

Clean plates were coated with dye using one of three methods. These were: (1) dropping a few drops of solution onto a piece of lens tissue held on top of the plate, and waiting for the solvent to evaporate: which we refer to as drop coating, (2) drop-and-drag wiping, where the dropped solution is pulled along the surface by pulling the lens tissue, and (3) dip coating, where the plate is dipped into the solution and removed slowly. The different methods of coating were found to be virtually identical in the results produced, except in the amount of dye that was deposited on the surface. Methods (1) and (2) were preferred, since the techniques were simpler and could be performed *in-situ*. For consistency, all of the results presented in this paper were obtained using method (1). Great

care was taken to ensure that the plate was completely cleaned between successive coatings, since it was found that insufficient cleaning led to accumulation of dye and dust.

III. Results

Plots of ringdown time *versus* wavelength for an empty cavity, a blank plate, and a plate coated with malachite green are shown in Fig. 2. If the ringdown time for the empty cavity is τ_0 and the ringdown time for the blank plate is τ_b , we may calculate the total losses due to the blank plate a_b as

$$a_b = \frac{l}{c} \left(\frac{\tau_0 - \tau_b}{\tau_0 \tau_b} \right), \quad (2)$$

where l is the length of the cavity (0.75 m), c is the speed of light, and a_b is the dimensionless fractional loss per pass. The typical losses for a blank plate are plotted against wavelength in Fig. 2, and we see that the losses are nearly constant at around 220 ppm per pass. A similar expression can be used to calculate the losses of the coated dye relative to the blank plate

$$a = \frac{l}{c} \left(\frac{\tau_b - \tau}{\tau_b \tau} \right) = \varepsilon c_s \ln 10, \quad (3)$$

where τ is the ringdown time for the coated plate, ε is the molar (decadic) absorption coefficient, and c_s the surface concentration of the dye molecules. For example, coating with 25.7 μM malachite green solution, we measured $a = 0.00159$ at 620 nm. The molar extinction coefficient of malachite green in acetone is $\varepsilon_{620} = 8070 \text{ m}^2 \text{ mol}^{-1}$, and we make the assumption that this value is not significantly different for the coated plate. Using these values we estimate the surface concentration of molecules $c_s = 8.56 \times 10^{-8} \text{ mol m}^{-2}$. By knowing the beam size in the cavity, we can also estimate the total number of molecules illuminated. The size of the beam in the cavity was measured to be 1.5 mm in diameter.¹³ With the Brewster plate at $\Theta_B = 56.5^\circ$, we estimate the area of the illuminated ellipse on the plate surface to be $1.02 \times 10^{-6} \text{ m}^2$. Using this area with value for c_s given above, we estimate that a total of 5.26×10^{10} molecules are illuminated on the surface of the plate.

The total number of photons n_{phot} in the cavity during one decay can be estimated from the PMT signal:^{14,15}

$$n_{\text{phot}} = \frac{2\tau_0 V_{\text{scope}} \Delta_{\text{TTS}}}{RGQI_c}, \quad (4)$$

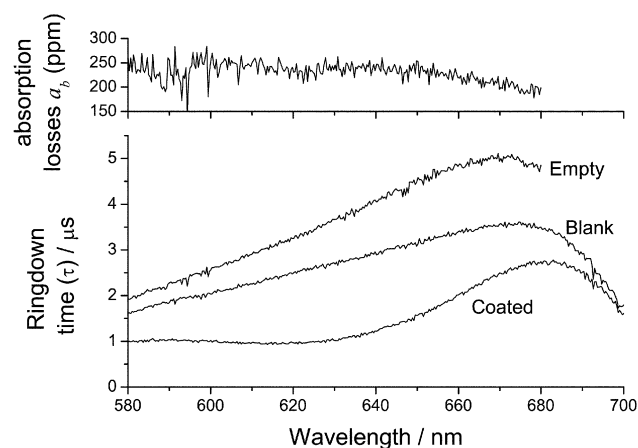


Fig. 2 Bottom panel: typical ringdown times as a function of wavelength for the empty cavity, and a cavity with blank and coated plates aligned at Brewster's angle (drop coating using 25.7 μM malachite green in acetone). Top panel: typical losses a_b (parts per million per pass) for a blank plate as a function of wavelength.

where $R = 50 \Omega$ is the resistive load at the output of the PMT, $G = 7.64 \times 10^4$ is the total gain of the PMT and the fast pre-amplifier, Q is the wavelength dependent quantum efficiency of the PMT ($Q = 0.084$ at 620 nm), V_{scope} is the initial decay voltage as measured on the oscilloscope, PMT current $I_e = 1.602 \times 10^{-10}$ electrons per nanosecond, $\Delta_{\text{TTS}} = 22$ ns is the transit time spread of the PMT, and $\tau_0 \sim 3250$ ns is the empty cavity decay time. The factor of 2 in the equation accounts for the fact that our PMT only measures the photon flux at one mirror. Using eqn. (4), we estimate $n_{\text{phot}} = 2.8 \times 10^7$ photons per decay. Comparing the estimated number of photons to our estimate of the number of molecules illuminated for malachite green, we see that there are several orders of magnitude more dye molecules than photons, and we are confident that the absorption is far from saturated.

A plot of absorption *versus* wavelength obtained by BACRDS for a solution of 25.7 μM malachite green in acetone drop-coated onto a plate is shown in Fig. 3. The borosilicate surface consists of negatively charged silyl Si-O⁻ end-groups, and the positively charged dye molecules are attracted to the surface. Also shown in Fig. 3 is a visible spectrum of the coating precursor solution as obtained using a conventional absorption spectrometer. The BACRDS spectrum shows a slight blue-shift in the maximum of the absorption, and increased absorption either side of the maximum. Identical absorption curves were obtained after cleaning and re-coating, and by using different plates. The blue-shift may be due to a solvatochromic perturbation resulting from the polar nature of the borosilicate surface, or simply a shift due to the increased absorption at shorter wavelengths. The broadening of the absorption feature is indicative of formation of dimers of malachite green, which form new bands to the blue and red of the monomer peak.¹⁶ It is also possible that higher aggregates are formed, although the Zanker analysis of Yao *et al.* suggests that the absorption band at 580 nm can be assigned to the malachite green dimer. In the present study, we found that the shape of the absorption feature was nearly independent of the concentration of the precursor solution at concentrations from 3.8 μM to 122 μM , and we are led to believe that the surface itself induces the formation of the dimers, or higher aggregates. Clearly, dye-dye interactions are competitive with the surface interactions, presumably due to the highly polar rigid nature of the surface. Following Yao *et al.*,¹⁶ the concentration of dimers can be estimated using the absorptions at 580 nm and 620 nm, and comparing with dilute and concentrated solutions. We assume that the

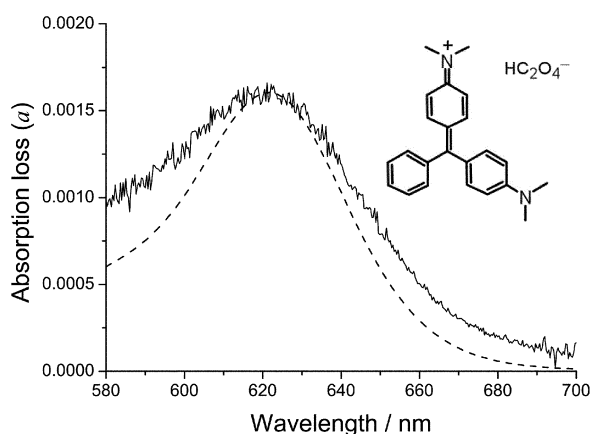


Fig. 3 Plot of absorption loss per pass (a) *versus* wavelength obtained by BACRDS for a drop coating using 25.7 μM malachite green in acetone (solid curve). A visible spectrum of the precursor solution is also shown (dashed line), which has been scaled to the BACRDS plot at 620 nm for comparison. The chemical structure of malachite green is also shown.

nature of the aggregation on the surface is the same as that in solution, and that dimers are not present in significant quantities in the dilute solution. Furthermore, the very rough approximation is made that dimers do not absorb at 620 nm.¹⁶ Yao *et al.* estimate the extinction coefficient of the dimer at 580 nm to be $\epsilon_{580}^{(d)} = 5160 \text{ m}^2 \text{ mol}^{-1}$. For the monomer $\epsilon_{620}^{(m)} = 8070 \text{ m}^2 \text{ mol}^{-1}$, and from the absorption spectrum of the dilute solution, we obtain $\epsilon_{580}^{(m)} = 3020 \text{ m}^2 \text{ mol}^{-1}$. At 580 nm, the absorption loss per pass $a_{580} = 9.7 \times 10^{-4}$ and at 620 nm $a_{620} = 0.0016$ (see Fig. 3). Using the extinction coefficients and the absorption values, we estimate the ratio of concentrations of dimers to monomers, $c_D/c_M = 0.36$.

Plots of absorption *versus* wavelength for oxazine 170 obtained by BACRDS for a series of coated acetone solutions are shown in Fig. 4, along with a visible spectrum of oxazine 170 in solution. The dye solution shows a peak in absorption at 618 nm, with a shoulder at shorter wavelength. The results are similar to those for malachite green, showing an absorption feature that is broadened with respect to the dye in solution. The shoulder at 580 nm is very strong, and appears to increase only slightly relative to the peak at 620 nm with increasing concentration of the precursor dye solution. The presence of the shoulder is again suggestive of the formation of aggregates, although care must be taken in making this assertion because oxazine 170 can lose a proton to form a molecular species with a broad absorption maximum around 500 nm.¹⁷ For this reason, absorption and fluorescence spectroscopy of oxazine 170 has been used as a method of determining the local environment or pH in films and glasses.¹⁸ The pK_a of oxazine 170 is $10.0 \pm 0.2 \text{ mol dm}^{-3}$ in aqueous solution, and it is unlikely that the surface can act as a sufficiently strong proton acceptor to produce significant quantities of the de-protonated molecule.¹⁷

Oxazine 1 has a similar structure to oxazine 170, but both amino end-groups consist of diethylamine groups, and the molecule does not readily lose a proton. Plots of oxazine 1 absorption obtained by BACRDS in comparison to absorption spectra of oxazine 1 in solution are shown in Fig. 5. The absorption shows a broadening of the main absorption peak, as was found for malachite green and oxazine 170. Aqueous and monohydric alcohols are known to enhance aggregate formation for oxazine 1, partly due to stabilization of

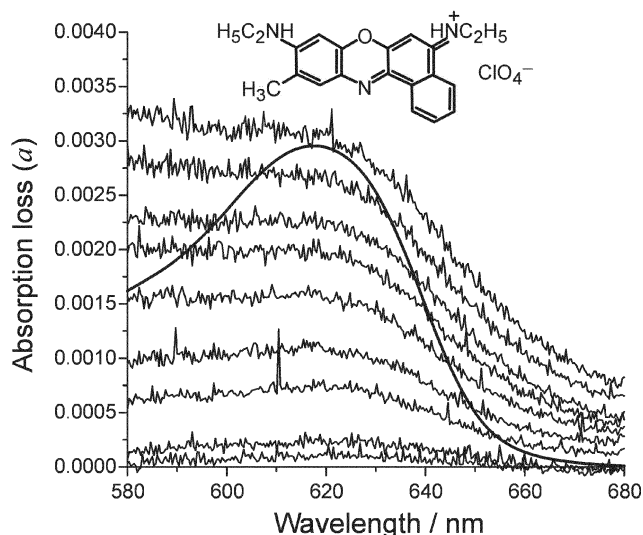


Fig. 4 Plot of absorption loss per pass (a) *versus* wavelength obtained by BACRDS for a series of coatings of oxazine 170 acetone solutions. The concentrations of the precursor dye solution (in acetone) from smallest to highest were 2.03, 4.06, 8.13, 16.3, 24.4, 32.5, 48.8, 65.0, and 130.0 μM . Also shown for comparison is a visible spectrum of oxazine 170 in solution (smooth curve).

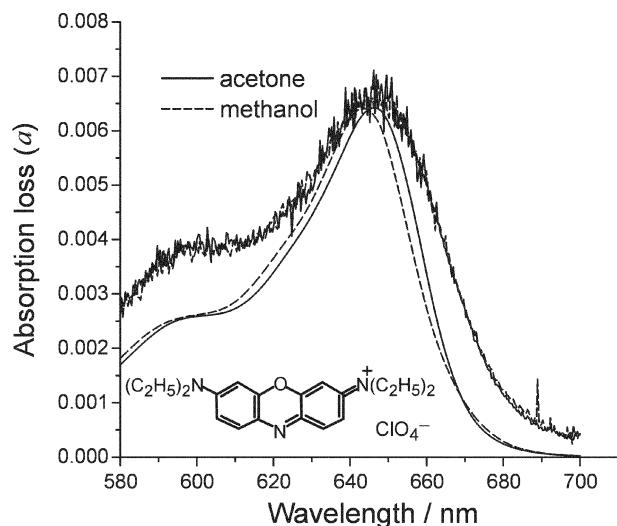


Fig. 5 Plot of absorption loss (a) versus wavelength obtained by BACRDS (solid lines) for coatings of $\sim 300 \mu\text{M}$ oxazine 1 solutions in acetone (solid) and methanol (dashed). Also shown for comparison are visible spectra of the precursor solutions (smooth curves). All of the data have been re-scaled to the BACRDS acetone results for direct comparison. Results obtained using more dilute ($\sim 9 \mu\text{M}$) solutions were almost identical to those shown, but had much lower signal to noise.

the solvent network.¹⁹ However, comparison with results for coating of plates from methanol solutions show the dimer formation at the surface appears to be independent of the solvent used: see Fig. 5. Visible spectra of concentrated ($\sim 300 \mu\text{M}$) and dilute ($\sim 9 \mu\text{M}$) oxazine 1 dye solutions were found to be almost identical. Aqueous solutions at these concentrations did show an absorption shoulder at 600 nm that increased with increasing concentration of the dye, becoming a small peak at higher concentrations ($\sim 320 \mu\text{M}$). Evidently the aqueous environment is less favorable to the dye molecules, resulting in aggregation. However, we were unable to make reproducible coatings with aqueous solutions using any of the coating methods available to us, so it was not possible to verify the effect of precursor aggregation on the BACRDS results.

Plots of the BACRDS absorption coefficient a versus the concentration of the coating solution for oxazine 170 (taken from Fig. 4) are shown in Fig. 6. The results at 580 nm and 620 nm are very similar, supporting the general observation that the shape of the absorption does not change much over

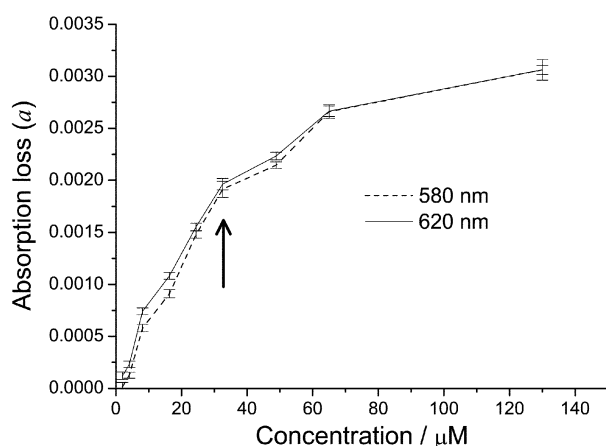


Fig. 6 Plot of absorption loss (a) versus concentration by BACRDS at 580 and 620 nm for the oxazine 170 data shown in Fig. 4. For easy comparison, the data at 580 nm have been scaled to match 620 nm data at the highest concentration. The arrow indicates approximate point of monolayer formation.

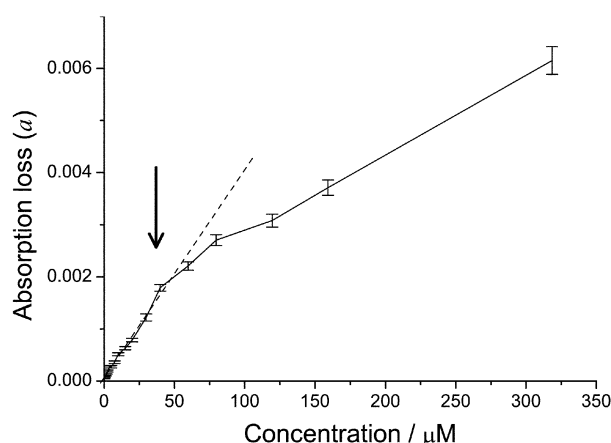


Fig. 7 Plot of absorption loss (a) versus concentration measured at a wavelength 646 nm by BACRDS for a series of coatings of oxazine 1 solutions in acetone. Each point represents the mean and single standard deviations from 50 repeated measurements. The dashed line shows a linear fit of the points up to the one marked with the arrow.

2 orders of magnitude of concentration of the precursor dye solution. The most striking feature of Fig. 6 is the deviation from linearity. At concentrations below $\sim 30 \mu\text{M}$, the absorption is directly proportional to concentration, and at higher concentrations, the absorption flattens out, *i.e.*, the absorption is lower than expected. Similar results were obtained for Rhodamine 640 (not shown) and oxazine 1 (Fig. 7). We believe that the linear portion of the plot of absorption (a) represents sub-monolayer formation of dye: at higher concentrations of dye, the number of surface sites available becomes saturated, and it becomes increasingly difficult to adsorb further layers on top of the first layer of molecules. This may be attributed to the polar interaction between the dye and the surface. With increasing coverage, the positive dye molecules effectively shield the negative charge of the silyl end-groups at the surface.

From Figs. 6 and 7, we assume that the points indicated with arrows represent the formation of 1 monolayer. For oxazine 170 and oxazine 1 this corresponds to solution concentrations of 32.5 and 39.8 μM , respectively. We note that Kemnitz *et al.* produced monolayers of Rhodamine by adsorption from 10^{-4} M aqueous solutions: very close to the value that we measure.²⁰ For oxazine 1, at the onset of monolayer coverage we observe $a = 0.00179$ at 646 nm. For our setup, assuming $\epsilon_{646} = 13000 \text{ m}^2 \text{ mol}^{-1}$, this corresponds to 3.60×10^{16} molecules m^{-2} . If we assume that the oxazine 1 molecules are approximately 100 \AA^2 rectangles tiled onto the surface, we roughly estimate a monolayer coverage of 10^{18} molecules m^{-2} . The monolayer coverage that we calculate is in good agreement, qualitatively, with the rough estimate of the number of sites available, with 0.036 of those sites filled by dye molecules.

The lowest absorption loss that we measured with confidence for oxazine 1 in the present experiment was $a = 5.79 \times 10^{-5}$, which would correspond to a coverage of 0.032 monolayers. This is comparable to the minimal detected coverage of 0.04 monolayers of iodine measured by Pipino *et al.*⁵

VI. Conclusions

Brewster angle cavity ringdown spectroscopy (BACRDS) has been demonstrated to be a simple and sensitive method for measuring absorption spectra of thin films coated onto planar substrates. Measured absorption spectra of coated films of malachite green and oxazine dyes in the visible region 580 to 700 nm show the presence of dye aggregates. The shape of the dye absorption feature appears to be roughly independent

of the concentration of the precursor coating solution. We have demonstrated the measurement of concentrations equivalent to monolayer and sub-monolayer coatings of dyes: the lowest coverage of oxazine 1 measured in the present work was estimated to be 0.032 monolayers. Significant improvements to sensitivity could be made by working at longer wavelengths where bulk scattering is reduced, and by using polished silica substrates to reduce scattering losses from the substrate interface. With these improvements, it is likely that the challenge in pushing the sensitivity limit would become the coating and sample-handling. The technique also shows promise for studies in which the surface is functionalized for selective attachment of species or chromatography.

Acknowledgements

AJA thanks the Royal Society for the award of a University Research Fellowship. We are grateful to Dr Andrew Orr-Ewing (University of Bristol) for a critical reading of the manuscript.

References

- 1 J. B. Paul and R. J. Saykally, *Anal. Chem.*, 1997, **69**, 287.
- 2 M. D. Wheeler, S. M. Newman, A. J. Orr-Ewing and M. N. R. Ashfold, *Faraday Trans. Chem. Soc.*, 1998, **94**, 337.
- 3 G. Berden, R. Peeters and G. Meijer, *Int. Rev. Phys. Chem.*, 2000, **19**, 565.
- 4 A. C. R. Pipino, J. W. Hudgens and R. E. Huie, *Rev. Sci. Instrum.*, 1997, **68**, 2978.
- 5 A. C. R. Pipino, J. W. Hudgens and R. E. Huie, *Chem. Phys. Lett.*, 1997, **280**, 104.
- 6 A. C. R. Pipino, *Phys. Rev Lett.*, 1999, **83**, 3093; A. C. R. Pipino, *Appl. Opt.*, 2000, **39**, 1449.
- 7 R. Engeln, G. von Helden, A. J. A. van Roij and G. Meijer, *J. Chem. Phys.*, 1999, **110**, 2732.
- 8 S. L. Logunov, *Appl. Opt.*, 2001, **40**, 1570.
- 9 D. Kleine, J. Lauterbach, K. Kleinermanns and P. Hering, *Appl. Phys. B*, 2001, **72**, 249.
- 10 S. Xu, G. Sha and J. Xie, *Rev. Sci. Instrum.*, 2002, **73**, 255.
- 11 A. J. Hallock, E. S. F. Berman and R. N. Zare, *Anal. Chem.*, 2002, **74**, 1741.
- 12 G. R. Fowles, *Introduction to Modern Optics*, Dover, New York, 1975.
- 13 Our estimate was made by adjusting an iris at the center of the cavity and observing changes in the ringdown time: and is larger than might be expected from the lowest-order transverse mode: see S. Spuler and M. Linne, *Appl. Opt.*, 2002, **41**, 2858. We did not match the mode of the laser pulse to the cavity: the large beam diameter may be attributed to excitation of higher-order transverse modes.
- 14 H. Naus, I. H. M. van Stokkum, W. Hogervorst and W. Ubachs, *Appl. Opt.*, 2001, **40**, 4416.
- 15 *Photomultiplier Tubes: Basics and Applications*, Hamamatsu Photonics KK, Japan, 2nd edn., 1999.
- 16 H. Yao, Y. Inoue, H. Ikeda, K. Nakatani, H.-B. Kim and N. Kitamura, *J. Phys. Chem.*, 1996, **100**, 1494.
- 17 R. Gvishi and R. Reisfeld, *Chem. Phys. Lett.*, 1989, **156**, 181.
- 18 M. Eyal, R. Gvishi and R. Reisfeld, *J. Phys.*, 1987, **48**, C7–423.
- 19 Y. P. Morozova and E. B. Zhigalova, *Russ. J. Phys. Chem.*, 1982, **56**, 1526.
- 20 K. Kemnitz, N. Tamai, I. Yamakazi, N. Nakashima and K. Yoshihara, *J. Phys. Chem.*, 1986, **90**, 5094.